

A model of the effect of collisions on QCD plasma instabilities

Björn Schenke,¹ Michael Strickland,² Carsten Greiner,¹ and Markus H. Thoma³

¹*Institut für Theoretische Physik
Johann Wolfgang Goethe - Universität Frankfurt
Max-von-Laue-Straße 1, D-60438 Frankfurt am Main, Germany*

²*Frankfurt Institute for Advanced Studies
Johann Wolfgang Goethe - Universität Frankfurt
Max-von-Laue-Straße 1, D-60438 Frankfurt am Main, Germany*

³*Max-Planck-Institute for Extraterrestrial Physics
P.O. Box 1312, 85741 Garching, Germany*

We study the effect of including a BGK collisional kernel on the collective modes of a QCD plasma which has a hard-particle distribution function which is anisotropic in momentum space. We calculate dispersion relations for both the stable and unstable modes and show that the addition of hard particle collisions slows the rate of growth of QCD plasma unstable modes. We also show that for any anisotropy there is an upper limit on the collisional frequency beyond which no instabilities exist. Estimating a realistic value for the collisional frequency for $\alpha_s \sim 0.2 - 0.4$ we find that for the large-anisotropy case which is relevant for the initial state of matter generated by free streaming in heavy-ion collisions that the collisional frequency is below this critical value.

PACS numbers: 11.15.-q, 11.10.Wx, 52.35.Qz

I. INTRODUCTION AND MOTIVATION

The ultrarelativistic heavy ion collision experiments ongoing at the Relativistic Heavy Ion Collider (RHIC) at Brookhaven National Laboratory (BNL) and planned at the Large Hadron Collider (LHC) at CERN study nuclear matter under extreme conditions. A main point of interest is the identification and investigation of a phase transition to the quark-gluon plasma (QGP). If it is created, the QGP is expected to expand, cool and finally hadronize. Whether or not it is possible to apply a thermodynamic description of the created system in its later stages of evolution depends on whether it thermalizes fast enough. RHIC data indicate that such a rapid thermalization does occur [1, 2, 3], in contradiction to leading order perturbation theory estimates. Therefore, many recent works have been dedicated to the explanation of how the fast thermalization is achieved. One possibility is the assumption of a strongly coupled QGP [4, 5]. In other approaches [6] the process of particle production leads to momentum distributions of the equilibrium form immediately, without any secondary processes needed. However it is not explained how the equilibrium state is maintained when the system is driven out of equilibrium by free streaming. Secondary processes are certainly necessary to explain this. Within recent transport theory approaches, the inclusion of particle production and absorption via $2 \leftrightarrow 3$ pQCD bremsstrahlung processes speeds up the equilibration significantly [7] as compared to equilibration solely driven by perturbative binary collisions.

Here we will concentrate on the role of non-equilibrium QCD collective modes in the isotropization and thermalization of the system as investigated in [8, 9, 10, 11, 12, 13, 14, 15, 16, 17, 18, 19, 20, 21, 22] (for a recent review see [23]). In these approaches the QGP is assumed to be homogeneous and stationary, but anisotropic in momentum space, such that kinetic instabilities can occur. They are initiated either by charge or current fluctuations. In the first case, the electric field is parallel to the wave vector \mathbf{k} ($\mathbf{E} \parallel \mathbf{k}$), while in the second case the field is perpendicular to \mathbf{k} ($\mathbf{E} \perp \mathbf{k}$). This is why the corresponding instabilities are called longitudinal and transverse, respectively. Since the electric field plays a crucial role in the generation of longitudinal modes, they are also called electric, while the transverse modes are called magnetic. The magnetic mode known as the filamentation- or Weibel-instability [24] appears to be relevant for the QGP [8, 9, 10], created in heavy ion collisions.

The instabilities are found to have a significant effect on the system's evolution, leading to a faster isotropization and equilibration. The equilibration due to instabilities only happens indirectly, because the instabilities driven isotropization is a mean-field reversible process, which does not produce entropy. However, parton momentum distributions are influenced by the isotropization, which speeds up the equilibration. Collisions, being responsible for the dissipation are needed to reach the equilibrium state of maximum entropy. All calculations so far have been carried out at leading order in perturbation theory, such that collisions among the hard particles that enter at higher orders in g could be neglected. However, in heavy ion collision experiments at the RHIC and LHC the couplings expected are of the order $\alpha_s \sim 0.2 - 0.4$ and higher order terms will be important. Hence, collisions can not simply

be neglected and their effect on the system's evolution, particularly on the collective modes, has to be investigated. We expect that the inclusion of collisional damping will decrease the instability growth rate, however, one would like to make this statement quantitative and say precisely by how much the growth rate is reduced. This is the main objective of the present work in that we give a first quantitative estimate of how the collisions affect the dispersion relations of the collective modes and the growth of instabilities in particular. To achieve this, we introduce a model for the inclusion of collisions based on the Vlasov equations for QCD combined with a BGK-type [25] collision term. The regarded anisotropic distributions are derived from an isotropic one by contracting the hard particle distribution function along a preferred direction. We concentrate on the case in which the direction of anisotropy is parallel to the wave vector of the regarded collective mode, because in this case the growth rate of the magnetic instability is maximal and analytic expressions for the structure functions can be found. For any such distribution we find that the growth rate of instabilities decreases approximately linearly with increasing collision rate and there exists a critical collision rate above which instabilities cease to exist.

The current work is organized as follows: In Section II we briefly review the kinetic approach in the collisionless case. We introduce the model for the inclusion of collisions in Section III, which closes with the final result for the self energy of the collective modes. Section IV briefly reviews the procedure for finding the dispersion relations and in Section V we derive the structure functions and dispersion relations for the specified anisotropic systems. Final results for the dispersion relations of the stable modes including collisions are given in Section VI while the influence of collisions on the unstable modes is shown in Section VII. In Section VIII we discuss further the results and attempt to estimate the numerical value of the collisional frequency. In Section IX we conclude and give an outlook.

II. COLLISION FREE TRANSPORT EQUATIONS

In the kinetic theory approach [8, 9, 10, 11, 13, 26, 27, 28, 29, 30] gluons, quarks and antiquarks are described by their phase space densities, given by the gauge covariant Wigner functions $n^i(p, X)$, with $i \in \{g, q, \bar{q}\}$. To obtain the linearized transport equations we expand $n^i(p, X) = n^i(\mathbf{p}) + \delta n^i(p, X)$. After a gauge covariant gradient expansion of the generalized QCD-Kadanoff-Baym equations for the quark and gluon Green functions, the linearized equations of motion read [8, 9, 10, 11, 13, 26, 27, 28, 29, 30]

$$[V \cdot D_X, \delta n^i(p, X)] + g\theta_i V_\mu F^{\mu\nu}(X) \partial_\nu^{(p)} n^i(\mathbf{p}) = 0, \quad (1)$$

where $V = (1, \mathbf{v})$ with $\mathbf{v} = \mathbf{p}/|\mathbf{p}|$ and $\theta_g = \theta_q = 1$ and $\theta_{\bar{q}} = -1$. $D_X = \partial_X + igA(X)$ is the covariant derivative with the soft gauge field $A^\mu = A_a^\mu T^a$ or $A^\mu = A_t^\mu t^a$ in the gluon and quark equations of motion, respectively. The gluon field strength tensor is given by $F^{\mu\nu} = \partial^\mu A^\nu - \partial^\nu A^\mu - ig[A^\mu, A^\nu]$. Eq. (1) holds for each particle species, with the color neutral background fields $n^{q/\bar{q}}(\mathbf{p}) = f^{q/\bar{q}}(\mathbf{p})I$ and $n^g(\mathbf{p}) = f^g(\mathbf{p})\mathcal{I}$. I and \mathcal{I} are unit matrices in the fundamental and adjoint representation, respectively. The scalar functions $f^{q/\bar{q}}(\mathbf{p})$ and $f^g(\mathbf{p})$ are found by projection:

$$\begin{aligned} f^{q/\bar{q}}(\mathbf{p}) &= \frac{1}{N_c} \text{Tr} \left[n^{q/\bar{q}}(p, X) \right], \\ f^g(\mathbf{p}) &= \frac{1}{N_c^2 - 1} \text{Tr} [n^g(p, X)]. \end{aligned} \quad (2)$$

The induced fluctuations $\delta n^{q/\bar{q}}(p, X) = \delta f_b^{q/\bar{q}}(p, X) t^b$ and $\delta n^g(p, X) = \delta f_b^g(p, X) T^b$, with the generators t_b and T_b in the fundamental and adjoint representation, respectively, are assumed to be much smaller than the colorless background terms. The scalar functions $\delta f_a^i(p, X)$ again follow by projection:

$$\begin{aligned} \delta f_a^{q/\bar{q}}(p, X) &= 2 \text{Tr} \left[t_a n^{q/\bar{q}}(p, X) \right], \\ \delta f_a^g(p, X) &= \frac{1}{N_c} \text{Tr} [T_a n^g(p, X)]. \end{aligned} \quad (3)$$

The induced current for each color channel reads [11, 30]

$$J_{\text{ind } a}^{\mu} = g \int_{\mathbf{p}} V^\mu \left\{ 2N_c \delta f_a^g(p, X) + N_f [\delta f_a^q(p, X) - \delta f_a^{\bar{q}}(p, X)] \right\}, \quad (4)$$

with

$$\int_{\mathbf{p}} := \int \frac{d^3 p}{(2\pi)^3}. \quad (5)$$

When we concentrate on the soft scale $k \sim gT \ll T$, the first scale at which collective motion appears, we can neglect terms of subleading order in g and the theory becomes effectively Abelian.¹ Now all color channels decouple in Eq. (1) and we find separate solutions for each $\delta f_a^i(p, X)$. After Fourier transformation the total induced current (4) becomes [11]

$$J_{\text{ind } a}^\mu(K) = g^2 \int_{\mathbf{p}} V^\mu \partial_{(p)}^\beta f(\mathbf{p}) \left(g_{\gamma\beta} - \frac{V_\gamma K_\beta}{K \cdot V + i\epsilon} \right) A_a^\gamma(K) + \mathcal{O}(g^3 A^2), \quad (6)$$

where $K = (\omega, \mathbf{k})$ and the effective background phase space density is given by

$$f(\mathbf{p}) = 2N_c f^g(\mathbf{p}) + N_f [f^q(\mathbf{p}) + f^{\bar{q}}(\mathbf{p})]. \quad (7)$$

Functional differentiation of the induced current with respect to the gauge field A_ν and taking $A_\nu \rightarrow 0$ leads to the gluon self-energy, which equals the one which can be obtained by a hard-loop resummation within the diagrammatic approach in the collisionless case.

III. INCLUSION OF COLLISIONS

In the effectively Abelian limit, introduced in Section II, the equation of motion (1) holds for each color channel separately, such that we can write

$$V \cdot \partial_X \delta f_a^i(p, X) + g\theta_i V_\mu F_a^{\mu\nu}(X) \partial_\nu^{(p)} f^i(\mathbf{p}) = \mathcal{C}_a^i(p, X), \quad (8)$$

where we have included the collision term \mathcal{C}_a^i , given by

$$\mathcal{C}_a^i(p, X) = -\nu \left[f_a^i(p, X) - \frac{N_a^i(X)}{N_{\text{eq}}^i} f_{\text{eq}}^i(|\mathbf{p}|) \right], \quad (9)$$

with $f_a^i(p, X) = f^i(\mathbf{p}) + \delta f_a^i(p, X)$. This BGK-type collision term [25] describes how collisions equilibrate the system within a time proportional to ν^{-1} . Here we will assume that the collision rate ν is independent of momentum and particle species, however, these assumptions are easily relaxed. Note that these collisions are not color-rotating. The particle numbers are given by

$$N_a^i(X) = \int_{\mathbf{p}} f_a^i(p, X), \quad N_{\text{eq}}^i = \int_{\mathbf{p}} f_{\text{eq}}^i(|\mathbf{p}|) = \int_{\mathbf{p}} f^i(\mathbf{p}). \quad (10)$$

We note that the difference between the BGK collisional kernel (9) and the conventional relaxation-time approximation (RTA) is the multiplication of the second term in brackets by the ratio of the density over the equilibrium density. RTA simply takes the difference of the distribution function and the equilibrium distribution function implicitly setting this ratio to one. The advantage of the BGK kernel over an RTA kernel lies in the fact that the number of particles is instantaneously conserved by the BGK collisional-kernel, i.e., that

$$\int_{\mathbf{p}} \mathcal{C}_a^i(p, X) = 0. \quad (11)$$

This simply states that the collisions can only occur if a particle is present and that only the momentum of the particles will change as a result, not the particle number. This condition is violated by RTA. In addition, Ref. [31] showed that after a simple modification the BGK collisional-kernel covariantly conserves the color current.

The inclusion of a BGK collisional kernel allows for simulation of the effect of binary collisions with substantial momentum transfer and is merely an approximation for collisions between the hard charged particles in a hot quark-gluon plasma. However, in our opinion it is a reasonable way to yield a first quantitative answer to the question of how collisions among hard particles affect the collective modes of QCD. The effects of such a collision term on the dispersion relations in the ultrarelativistic case for an isotropic system were investigated in [32]. For now the collision

¹ This strictly only occurs at leading order in g . The induced current also contains terms of higher order in g (and A), which correspond to the non-Abelian self-interactions of the soft gauge field. Here we are looking at the self-energy, so that we can ignore these.

rate ν is taken to be a free parameter and we postpone the estimation of its magnitude to the discussions at the end of this paper.

Using (10) we can write

$$V \cdot \partial_X \delta f_a^i(p, X) + g\theta_i V_\mu F_a^{\mu\nu}(X) \partial_\nu^{(p)} f^i(\mathbf{p}) = -\nu \left[f^i(\mathbf{p}) + \delta f_a^i(p, X) - \left(1 + \frac{\int_{\mathbf{p}} \delta f_a^i(p, X)}{N_{\text{eq}}^i} \right) f_{\text{eq}}^i(|\mathbf{p}|) \right]. \quad (12)$$

Solving for $\delta f_a^i(p, X)$ and Fourier-transforming leads to the result for the linearized induced current by each particle species i (see Appendix A):

$$\begin{aligned} J_{\text{ind } a}^\mu(K) &= g^2 \int_{\mathbf{p}} V^\mu \partial_{(p)}^\beta f^i(\mathbf{p}) \mathcal{M}_{\gamma\beta}(K, V) D^{-1}(K, \mathbf{v}, \nu) A_a^\gamma(K) + g\nu \mathcal{S}^i(K, \nu) \\ &\quad + g \frac{i\nu}{N_{\text{eq}}^i} \int_{\mathbf{p}} V^\mu f_{\text{eq}}^i(|\mathbf{p}|) D^{-1}(K, \mathbf{v}, \nu) \\ &\quad \times g \left[\int_{\mathbf{p}'} \partial_{(p')}^\beta f^i(\mathbf{p}') \mathcal{M}_{\gamma\beta}(K, V') D^{-1}(K, \mathbf{v}', \nu) A_a^\gamma(K) + g\nu \mathcal{S}^i(K, \nu) \right] \mathcal{W}_i^{-1}(K, \nu), \end{aligned} \quad (13)$$

with

$$\mathcal{M}_{\gamma\beta}(K, V) := g_{\gamma\beta}(\omega - \mathbf{k} \cdot \mathbf{v}) - V_\gamma K_\beta, \quad (14)$$

$$D(K, \mathbf{v}, \nu) := \omega + i\nu - \mathbf{k} \cdot \mathbf{v}, \quad (15)$$

$$\mathcal{S}^i(K, \nu) := \theta_i \int_{\mathbf{p}} V^\mu [f^i(\mathbf{p}) - f_{\text{eq}}^i(|\mathbf{p}|)] D^{-1}(K, \mathbf{v}, \nu), \quad (16)$$

and

$$\mathcal{W}_i(K, \nu) := 1 - \frac{i\nu}{N_{\text{eq}}^i} \int_{\mathbf{p}} f_{\text{eq}}^i(|\mathbf{p}|) D^{-1}(K, \mathbf{v}, \nu). \quad (17)$$

The total induced current is given by $J_{\text{ind } a}^\mu(K) = 2N_c J_{\text{ind } a}^{g\mu}(K) + N_f [J_{\text{ind } a}^{q\mu}(K) + J_{\text{ind } a}^{\bar{q}\mu}(K)]$. It can be simplified due to the fact that the integrals over f_{eq}^i in Eq. (13) are independent of the particle species:

$$\begin{aligned} \frac{1}{N_{\text{eq}}^i} \int_{\mathbf{p}} f_{\text{eq}}^i(|\mathbf{p}|) D^{-1}(K, \mathbf{v}, \nu) &= \int \frac{d\Omega}{4\pi} D^{-1}(K, \mathbf{v}, \nu), \\ \frac{1}{N_{\text{eq}}^i} \int_{\mathbf{p}} V^\mu f_{\text{eq}}^i(|\mathbf{p}|) D^{-1}(K, \mathbf{v}, \nu) &= \int \frac{d\Omega}{4\pi} V^\mu D^{-1}(K, \mathbf{v}, \nu), \end{aligned} \quad (18)$$

where $d\Omega = \sin\theta d\theta d\varphi$. Assuming equal distributions for quarks and antiquarks, the full linearized induced current reads

$$\begin{aligned} J_{\text{ind } a}^\mu(K) &= g^2 \int_{\mathbf{p}} V^\mu \partial_{(p)}^\beta f(\mathbf{p}) \mathcal{M}_{\gamma\beta}(K, V) D^{-1}(K, \mathbf{v}, \nu) A_a^\gamma + 2N_c g\nu \mathcal{S}^g(K, \nu) \\ &\quad + g^2 (i\nu) \int \frac{d\Omega}{4\pi} V^\mu D^{-1}(K, \mathbf{v}, \nu) \int_{\mathbf{p}'} \partial_{(p')}^\beta f(\mathbf{p}') \mathcal{M}_{\gamma\beta}(K, V') D^{-1}(K, \mathbf{v}', \nu) \mathcal{W}^{-1}(K, \nu) A_a^\gamma \\ &\quad + 2N_c g^2 (i\nu^2) \int \frac{d\Omega}{4\pi} V^\mu D^{-1}(K, \mathbf{v}, \nu) \mathcal{S}^g(K, \nu) \mathcal{W}^{-1}(K, \nu), \end{aligned} \quad (19)$$

where $\mathcal{W}(K, \nu) = 1 - i\nu \int \frac{d\Omega}{4\pi} D^{-1}(K, \mathbf{v}, \nu)$ and $f(\mathbf{p})$ as in Eq. (7). The self energy is obtained from Eq. (19) via

$$\Pi_{ab}^{\mu\nu}(K) = \frac{\delta J_{\text{ind } a}^\mu(K)}{\delta A_\nu^b(K)}, \quad (20)$$

resulting in

$$\begin{aligned} \Pi_{ab}^{\mu\nu}(K) &= \delta_{ab} g^2 \int_{\mathbf{p}} V^\mu \partial_\beta^{(p)} f(\mathbf{p}) \mathcal{M}^{\nu\beta}(K, V) D^{-1}(K, \mathbf{v}, \nu) \\ &+ \delta_{ab} g^2 (i\nu) \int \frac{d\Omega}{4\pi} V^\mu D^{-1}(K, \mathbf{v}, \nu) \int_{\mathbf{p}'} \partial_\beta^{(p')} f(\mathbf{p}') \mathcal{M}^{\nu\beta}(K, V') D^{-1}(K, \mathbf{v}', \nu) \mathcal{W}^{-1}(K, \nu), \end{aligned} \quad (21)$$

which is diagonal in color and can be shown to be transverse, i.e., $K_\mu \Pi^{\mu\nu} = K_\nu \Pi^{\mu\nu} = 0$. We will from now on omit the color indices of $\Pi^{\mu\nu}$. The terms in the induced current involving \mathcal{S}_ν drive the distribution into an isotropic equilibrium shape. They represent a parity conserving current and thus create a zero average electromagnetic field and therefore does not contribute to instability growth.

IV. DISPERSION RELATIONS

In the linear approximation, the current that is induced by the fluctuations can be expressed in terms of the self energy by

$$J_{\text{ind}1}^\mu(K) = \Pi^{\mu\nu}(K) A_\nu(K), \quad (22)$$

where $J_{\text{ind}}^\mu = J_{\text{ind}1}^\mu + J_{\text{ind}2}^\mu$ and $J_{\text{ind}2}^\mu$ is the parity conserving part of the current (19) that does not couple to the gauge field. Note that for a parity symmetric distribution as we use below, $J_{\text{ind}2}^\mu = 0$. Inserting this into Maxwell's equation

$$iK_\mu F^{\mu\nu}(K) = J_{\text{ind}1}^\nu + J_{\text{ext}}^\nu, \quad (23)$$

we obtain

$$[K^2 g^{\mu\nu} - K^\mu K^\nu + \Pi^{\mu\nu}(K)] A_\mu(K) = J_{\text{ext}}^\nu(K), \quad (24)$$

with the external current J_{ext}^ν . In the temporal axial gauge, where $A_0 = 0$, this becomes

$$[(k^2 - \omega^2) \delta^{ij} - k^i k^j + \Pi^{ij}(K)] E^j(K) = [\Delta^{-1}(K)]^{ij} E^j(K) = i\omega J_{\text{ext}}^i(K), \quad (25)$$

and the response of the system to the external source is given by

$$E^i(K) = i\omega \Delta^{ij}(K) J_{\text{ext}}^j(K). \quad (26)$$

The dispersion relations are obtained by finding the poles of the propagator $\Delta^{ij}(K)$.

V. SELF ENERGY AND PROPAGATOR IN AN ANISOTROPIC SYSTEM

So far, the distribution function $f(\mathbf{p})$ in Eq. (21) has not yet been specified. We assume that $f(\mathbf{p})$ can be obtained from any isotropic distribution function by rescaling one direction in momentum space by defining [14]

$$f(\mathbf{p}) = \sqrt{1 + \xi} f_{\text{iso}}(\mathbf{p}^2 + \xi(\mathbf{p} \cdot \hat{\mathbf{n}})), \quad (27)$$

for an arbitrary isotropic distribution function $f_{\text{iso}}(|\mathbf{p}|)$. Distributions like (27) with $\xi > 0$ are generated during a heavy-ion collision at times $\tau > \langle p_T \rangle^{-1}$. The direction of the anisotropy above is given by $\hat{\mathbf{n}}$ and $\xi > -1$ is an adjustable anisotropy parameter. $\xi > 0$ corresponds to a contraction of the distribution in the $\hat{\mathbf{n}}$ direction, whereas $-1 < \xi < 0$ represents a stretching of the distribution in the $\hat{\mathbf{n}}$ direction. The factor of $\sqrt{1 + \xi}$ ensures that the overall particle number is the same for both the anisotropic and the isotropic distribution function. With this particular distribution we are able to perform the radial part of the integrations involving $f(\mathbf{p})$ in Eq. (21) by changing variables to $\tilde{p}^2 = p^2(1 + \xi(\mathbf{v} \cdot \hat{\mathbf{n}})^2)$. The result is

$$\begin{aligned} \Pi^{ij}(K) &= m_D^2 \sqrt{1 + \xi} \int \frac{d\Omega}{4\pi} v^i \frac{v^l + \xi(\mathbf{v} \cdot \hat{\mathbf{n}}) n^l}{(1 + \xi(\mathbf{v} \cdot \hat{\mathbf{n}})^2)^2} [\delta^{jl}(\omega - \mathbf{k} \cdot \mathbf{v}) + v^j k^l] D^{-1}(K, \mathbf{v}, \nu) \\ &+ (i\nu) m_D^2 \sqrt{1 + \xi} \int \frac{d\Omega'}{4\pi} (v')^i D^{-1}(K, \mathbf{v}', \nu) \\ &\times \int \frac{d\Omega}{4\pi} \frac{v^l + \xi(\mathbf{v} \cdot \hat{\mathbf{n}}) n^l}{(1 + \xi(\mathbf{v} \cdot \hat{\mathbf{n}})^2)^2} [\delta^{jl}(\omega - \mathbf{k} \cdot \mathbf{v}) + v^j k^l] D^{-1}(K, \mathbf{v}, \nu) \mathcal{W}^{-1}(K, \nu), \end{aligned} \quad (28)$$

where

$$m_D^2 = -\frac{g^2}{2\pi^2} \int_0^\infty d\tilde{p} \tilde{p}^2 \frac{df_{\text{iso}}(\tilde{p}^2)}{d\tilde{p}}. \quad (29)$$

We now decompose the self energy into four structure functions, using the general tensor basis for an anisotropic system, developed in [14], such that

$$\Pi^{ij} = \alpha A^{ij} + \beta B^{ij} + \gamma C^{ij} + \delta D^{ij}, \quad (30)$$

where

$$A^{ij} = \delta^{ij} - k^i k^j / k^2, \quad B^{ij} = k^i k^j / k^2, \quad C^{ij} = \tilde{n}^i \tilde{n}^j / \tilde{n}^2, \quad D^{ij} = k^i \tilde{n}^j + k^j \tilde{n}^i, \quad (31)$$

with $\tilde{n}^i = A^{ij} n^j$ the part of n that is perpendicular to k , i.e., $\tilde{n} \cdot k = 0$. We determine the structure functions by taking the contractions:

$$k^i \Pi^{ij} k^j = k^2 \beta, \quad \tilde{n}^i \Pi^{ij} k^j = \tilde{n}^2 k^2 \delta, \quad \tilde{n}^i \Pi^{ij} \tilde{n}^j = \tilde{n}^2 (\alpha + \gamma), \quad \text{Tr} \Pi^{ij} = 2\alpha + \beta + \gamma. \quad (32)$$

In this basis, the inverse of the propagator in Eq. (25) can be written as

$$\Delta^{-1}(K) = (k^2 - \omega^2 + \alpha) \mathbf{A} + (\beta - \omega^2) \mathbf{B} + \gamma \mathbf{C} + \delta \mathbf{D}, \quad (33)$$

while the propagator itself is given by [14]:

$$\Delta(K) = \Delta_A (\mathbf{A} - \mathbf{C}) + \Delta_G [(k^2 - \omega^2 + \alpha + \gamma) \mathbf{B} + (\beta - \omega^2) \mathbf{C} - \delta \mathbf{D}], \quad (34)$$

with

$$\Delta_A^{-1}(K) = k^2 - \omega^2 + \alpha, \quad (35)$$

$$\Delta_G^{-1}(K) = (k^2 - \omega^2 + \alpha + \gamma)(\beta - \omega^2) - k^2 \tilde{n}^2 \delta^2. \quad (36)$$

Since the growth rate of the filamentation instability is the largest when the wave vector is parallel to the direction of the anisotropy, i.e., $\mathbf{k} \parallel \hat{\mathbf{n}}$ (see e.g. [14, 16, 33]), we concentrate on this particular case. Then

$$\mathbf{k} \cdot \mathbf{v} = k \hat{\mathbf{n}} \cdot \mathbf{v} = k \cos \theta, \quad (37)$$

and γ and $\tilde{n}^2 = 1 - (\mathbf{k} \cdot \hat{\mathbf{n}})^2$ vanish identically. To determine the poles of the propagator (34), and hence the dispersion relations, we are now left with two separate equations for the α - and β -mode, respectively:

$$\begin{aligned} k^2 - \omega^2 + \alpha &= 0, \\ \beta - \omega^2 &= 0. \end{aligned} \quad (38)$$

From Eqs. (32) we find α and β , which correspond to Π_T and $(\omega^2/k^2)\Pi_L$, respectively. The integrals can be solved analytically and the final results simplify to:

$$\begin{aligned} \alpha(\omega, k, \xi, \nu) &= \frac{m_D^2}{4} \frac{\sqrt{1+\xi}}{k(1+\xi z^2)^2} \left\{ (k(z^2 - 1) - iz\nu)(1 + \xi z^2) - (z^2 - 1)(kz(1 + \xi) - i\nu) \ln \left[\frac{z+1}{z-1} \right] \right. \\ &\quad \left. - \frac{i}{\sqrt{\xi}} [z\nu(1 + (3 + z^2(1 - \xi))\xi) + ik(1 - \xi + z^2(1 + \xi(6 + z^2(\xi - 1) + \xi)))] \arctan \sqrt{\xi} \right\}, \end{aligned} \quad (39)$$

$$\begin{aligned} \beta(\omega, k, \xi, \nu) &= m_D^2 \sqrt{1 + \xi} k (kz - i\nu)^2 \left\{ -2\sqrt{\xi}(1 + z^2\xi) + (1 + \xi) \left(2z\sqrt{\xi} \ln \left[\frac{z+1}{z-1} \right] + 2(z^2\xi - 1) \arctan \sqrt{\xi} \right) \right\} \\ &\quad \times \left(2\sqrt{\xi}(1 + z^2\xi)^2 k^2 \left(2k - i\nu \ln \left[\frac{z+1}{z-1} \right] \right) \right)^{-1}, \end{aligned} \quad (40)$$

where we abbreviate $z = (\omega + i\nu)/k$.

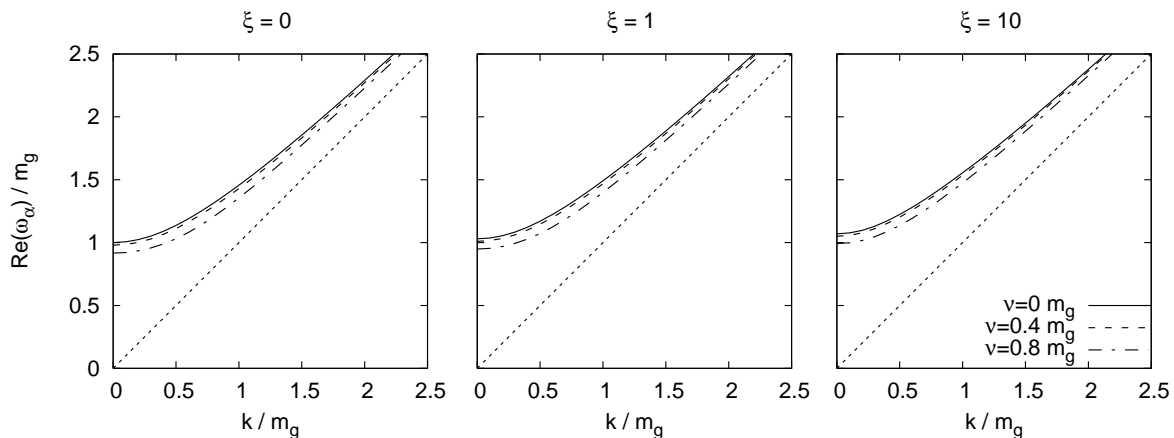


FIG. 1: Real part of the dispersion relation for the stable α -mode for an anisotropy parameter of $\xi = \{0, 1, 10\}$ and different collision rates in units of $m_g = m_D/\sqrt{3}$.

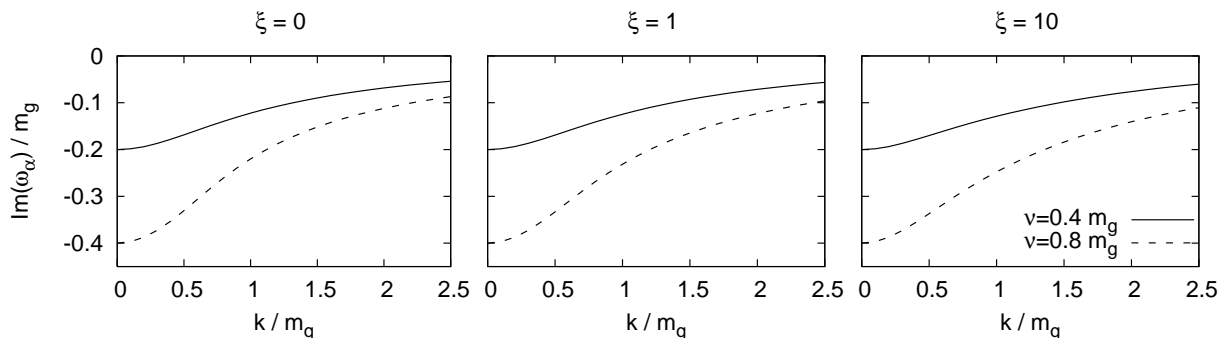


FIG. 2: Imaginary part of the dispersion relation for the stable α -mode for an anisotropy parameter of $\xi = \{0, 1, 10\}$ and different collision rates in units of $m_g = m_D/\sqrt{3}$.

VI. STABLE MODES

The dispersion relations for all modes are given by the solutions $\omega(k)$ of Eqs. (38). These solutions are found numerically for different values of the collision rate ν . The results for the stable transverse (α -) mode are shown in Figs. 1 and 2 for two anisotropic distributions, $\xi = 1$ and $\xi = 10$, together with the result for the isotropic case ($\xi = 0$). Note that the finite collision rate causes ω_α to become complex with a negative imaginary part corresponding to damping of these types of modes.

The effect of collisions on the stable longitudinal (β -) modes is more significant. The results are presented in Figs. 3 and 4. We find that for finite ν the dispersion becomes spacelike ($\text{Re}(\omega) < k$) at large k in contrast to the collisionless case, in which $\text{Re}(\omega) > k$ always holds. This behavior is responsible for the fact that the solution vanishes from the physical Riemann sheet above some finite k . This occurs precisely when the solution for ω_β reaches the cut between $-k$ and k at $-i\nu$.

It is however possible to find solutions on the unphysical Riemann sheets by replacing the logarithm in the structure function with its usual analytic continuation [16]:

$$\ln\left(\frac{z+1}{z-1}\right) = \ln\left(\left|\frac{z+1}{z-1}\right|\right) + i\left[\arg\left(\frac{z+1}{z-1}\right) + 2\pi N\right], \quad (41)$$

where N specifies the sheet number. The continuation of the solution to the lower Riemann sheets is shown in Figs. 5 and 6 for a collision rate of $\nu = 0.8 m_g \approx 0.46 m_D$ and different anisotropy parameters ξ . For smaller anisotropies the solution is found to converge to the light cone in an oscillating manner, while the imaginary part of ω oscillates around $\pm\nu$. Between $\xi = 2$ and $\xi = 3$ (for $\nu \approx 0.46 m_D$) this behavior changes qualitatively to the one shown in the case $\xi = 10$. With increasing k the real part of ω moves away from the light cone, while the imaginary part drops to

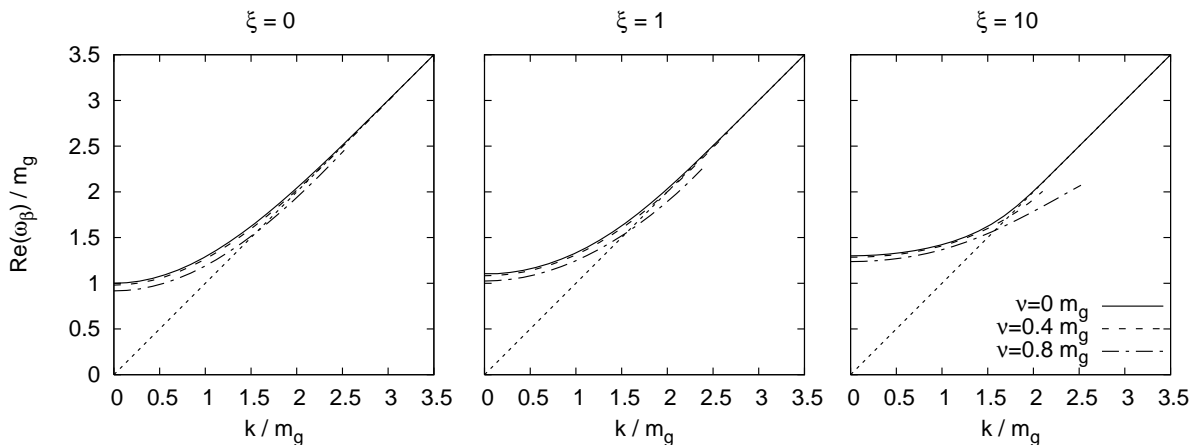


FIG. 3: Real part of the dispersion relation for the stable β -mode for an anisotropy parameter of $\xi = \{0, 1, 10\}$ and different collision rates in units of $m_g = m_D/\sqrt{3}$. Note that for finite ν there is a maximal k beyond which there is no solution. It vanishes when ω crosses the cut in the complex plane, which extends from $-k$ to $+k$ at $-i\nu$ (cf. Fig 4).

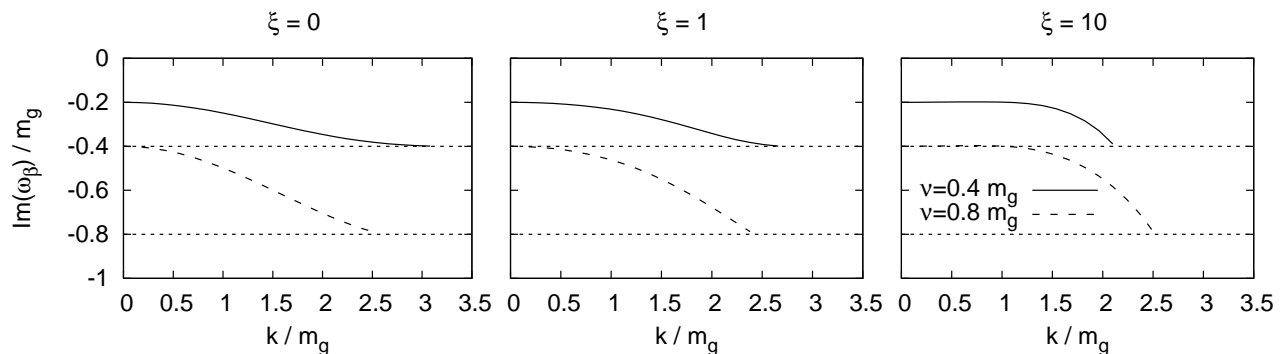


FIG. 4: Imaginary part of the dispersion relation for the stable β -mode for an anisotropy parameter of $\xi = \{0, 1, 10\}$ and different collision rates in units of $m_g = m_D/\sqrt{3}$. The solution vanishes, when ω crosses the cut in the complex plane, which extends from $-k$ to $+k$ at $-i\nu$ (indicated by the straight dotted line).

large negative values with the solution remaining on the $N = -1$ Riemann sheet, such that these modes are strongly damped.

VII. UNSTABLE MODES

Anisotropic momentum distributions cause kinetic instabilities. For the particular distribution (27) with $\hat{\mathbf{n}} \parallel \mathbf{k}$ and $\xi > 0$ there exists a magnetic instability, the so called filamentation or Weibel instability [24]. Its existence is due to a surplus of particles with momentum perpendicular (or close to perpendicular) to \mathbf{k} . These particles are trapped in the direction of \mathbf{k} by the background magnetic field and cause currents, which generate magnetic fields that add to the original one. Hence they contribute to instability, while all other particles have a stabilizing effect. (for a more detailed qualitative review of this scenario see [15]). In the isotropic case the stabilizing and destabilizing contributions cancel, such that no instability arises.

We now investigate how the inclusion of collisions as described in Section III affects the growth rates of these instabilities. Qualitatively one expects a decrease of the growth rates because the particles, which move perpendicular to \mathbf{k} , can scatter with other particles and will no longer be trapped. Other particles can gain a momentum close to perpendicular to \mathbf{k} and form a new contribution to the instability. However, since the collision term tends to randomize the momentum distribution, the growth of δf and the magnetic field is prevented. In order to describe this effect quantitatively, we solve Eq. (38) for purely imaginary ω and vary the collision rate ν . The solution $\omega(k) = i\Gamma(k)$ gives the growth rate $\Gamma(k)$. In the case that $\hat{\mathbf{n}} \parallel \mathbf{k}$ solutions like that only exist for the transverse (α -) mode. The

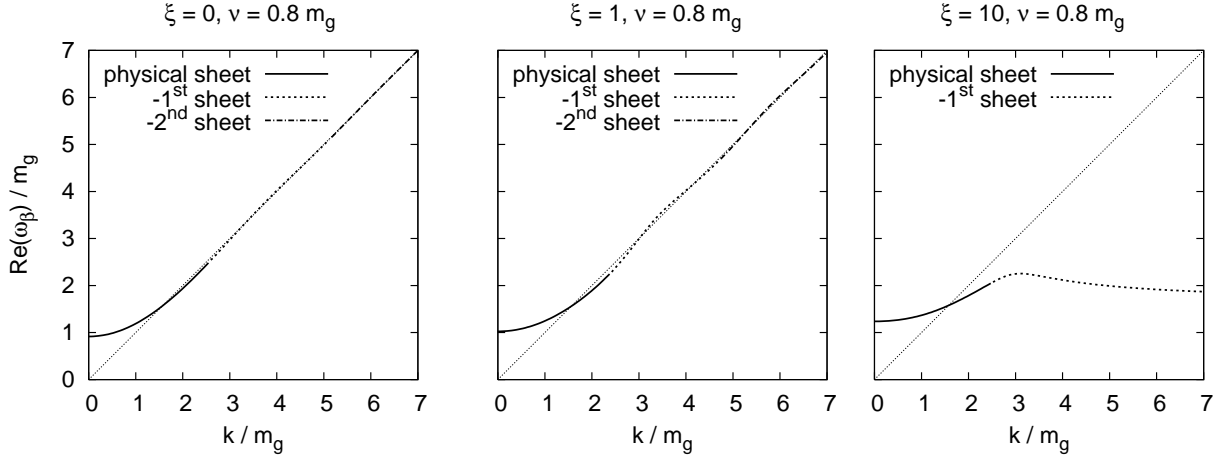


FIG. 5: Real part of the dispersion relation for the stable β -mode for an anisotropy parameter of $\xi = \{0, 1, 10\}$ and $\nu = 0.8 m_g$. It is shown how the solution continues on lower Riemann sheets.

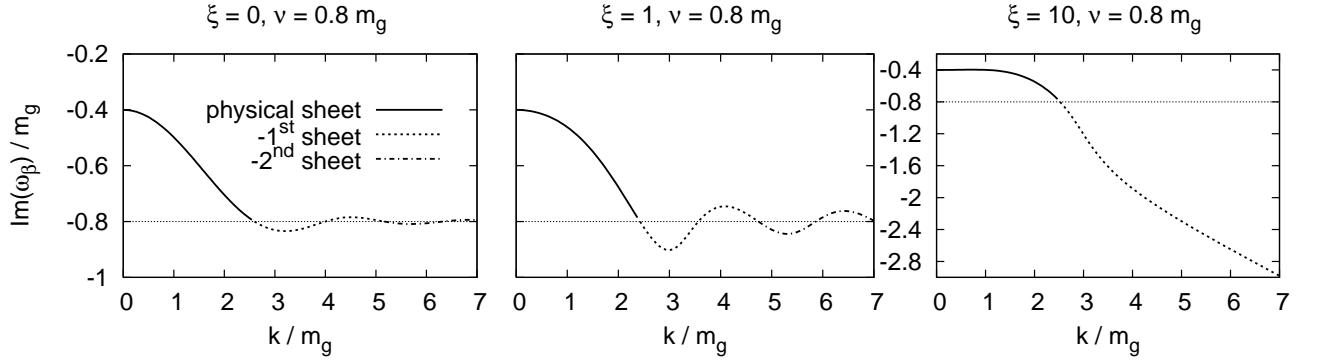


FIG. 6: Imaginary part of the dispersion relation for the stable β -mode for an anisotropy parameter of $\xi = \{0, 1, 10\}$ and $\nu = 0.8 m_g$. It is shown how the solution continues on lower Riemann sheets. Note the different scale for the third plot.

one with $\Gamma > 0$ corresponds to the filamentation instability. Results for different values of the collision rate ν are shown in Fig. 7 for $\xi = 1$ and in Fig. 8 for $\xi = 10$. The qualitatively expected effect is nicely reproduced. The growth rate decreases with an increasing collision rate as does the maximal wave number for an unstable mode. One can see that in the case where $\xi = 1$ already for ν being around 20% of the Debye mass, growth has completely turned into damping and no instability can evolve. For $\xi = 10$ the collision rate ν has to be slightly larger than 30% of the Debye mass in order to prevent growth of a collective mode. In order to find the wave number $k_{\max}(\xi, \nu)$ at which the unstable mode spectrum terminates, we take the limit $\omega \rightarrow 0$ to obtain

$$m_\alpha^2 = \lim_{\omega \rightarrow 0} \alpha = -\frac{m_D^2}{8} ik \frac{\sqrt{1+\xi}}{\sqrt{\xi}(k^2 - \nu^2 \xi)^2} \left\{ -2ik \sqrt{\xi}(k^2 - \nu^2 \xi) - 2\nu(k^2 + \nu^2) \xi^{3/2} \ln \left(1 - \frac{2k}{k - i\nu} \right) - 2ik [k^2(\xi - 1) + \nu^2 \xi(\xi + 3)] \arctan(\sqrt{\xi}) \right\}. \quad (42)$$

One of the solutions to the equation

$$k^2 + m_\alpha^2 = 0, \quad (43)$$

which is just the limit $\omega \rightarrow 0$ of the first of the Eqs. (38), is k_{\max} . Results for different ξ and ν are shown in Figs. 9 and 10. We find that for a given anisotropy parameter ξ , there exists a critical collision rate, above which instabilities can not occur. This is also true for the limit $\xi \rightarrow \infty$, as we will show in the following. Taking $\xi \rightarrow \infty$, Eq. (42) becomes

$$m_\alpha^2(\xi \rightarrow \infty) = -\frac{\pi}{8} m_D^2 \frac{k^2}{\nu^2}, \quad (44)$$

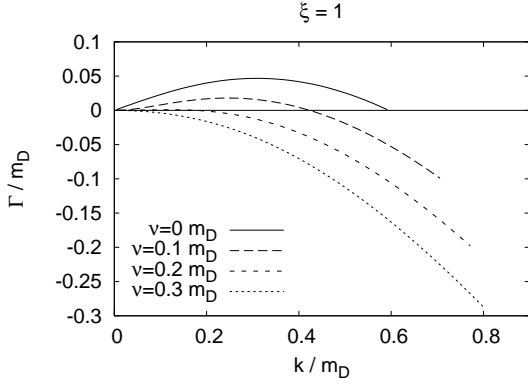


FIG. 7: Dependence of the growth rate Γ of the unstable transverse (α -) mode on the collision rate ν , for an anisotropy parameter $\xi = 1$.

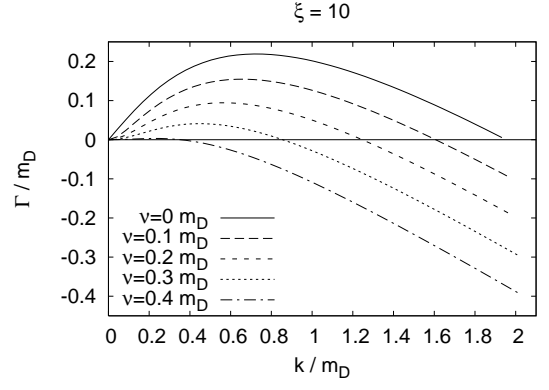


FIG. 8: Dependence of the growth rate Γ of the unstable transverse (α -) mode on the collision rate ν , for an anisotropy parameter $\xi = 10$.

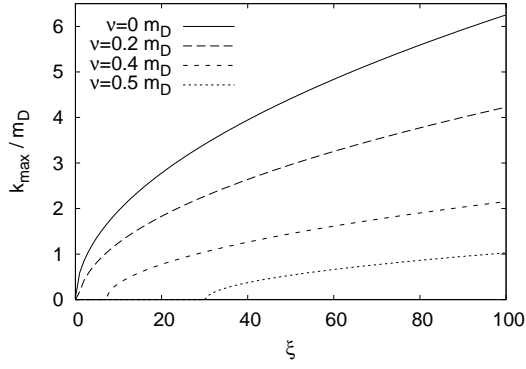


FIG. 9: k_{\max} of the maximally unstable mode as a function of the anisotropy parameter ξ for different values of ν . For given ν , the momentum anisotropy parameter must be above the critical value for instabilities to occur.

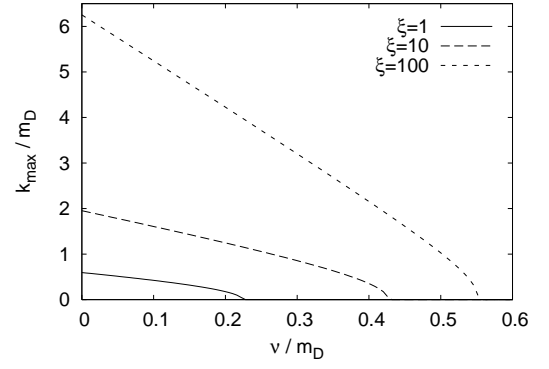


FIG. 10: k_{\max} of the maximally unstable mode as a function of the collision rate ν for given anisotropy parameter ξ . There exist ξ -dependent critical collision rates $\nu_{\max}(\xi)$ above which instabilities can not exist.

which together with Eq. (43) gives

$$k^2(\nu^2 - \frac{\pi}{8}m_D^2) = 0. \quad (45)$$

Apart from the result $k = 0$, this is solved by

$$\nu_{\max}(\xi \rightarrow \infty) = \sqrt{\frac{\pi}{8}}m_D \approx 0.6267 m_D = \Gamma_{\max}(\xi \rightarrow \infty), \quad (46)$$

the critical collision rate, above which even in the extremely anisotropic limit $\xi = \infty$ no instability can occur.

This is also visible in the plot of the growth rate $\Gamma_{\xi \rightarrow \infty}$, shown in Fig. 11. For $\nu = \nu_{\max}(\xi \rightarrow \infty)$ the growth rate becomes zero for all k , and for larger ν only damping occurs. In this case ($\xi = \infty$) the value of the maximal collision rate equals that of the maximal growth rate in the collisionless limit. This simply means that the instability vanishes completely at the point where the collisions damp at the same rate at which the instability grows. Note however that this relation is more complicated in general as shown in Fig. 12, where the dependence of the maximal growth rate on the collision rate is plotted. In order to make the instability vanish completely for any $\xi < \infty$, a collision rate larger than the maximal growth rate of the instability in the collisionless limit is needed.

VIII. DISCUSSIONS

In the body of the text the collisional frequency ν has been taken to be arbitrary. Because the inclusion of a BGK collisional term is a phenomenological model for the equilibration of a system and cannot be derived from

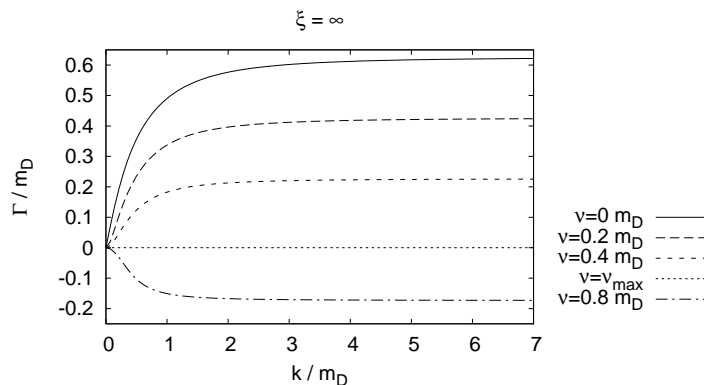


FIG. 11: Dependence of the growth rate Γ of the unstable transverse ($\alpha-$) mode on the collision rate ν , for the extremely anisotropic limit $\xi = \infty$.

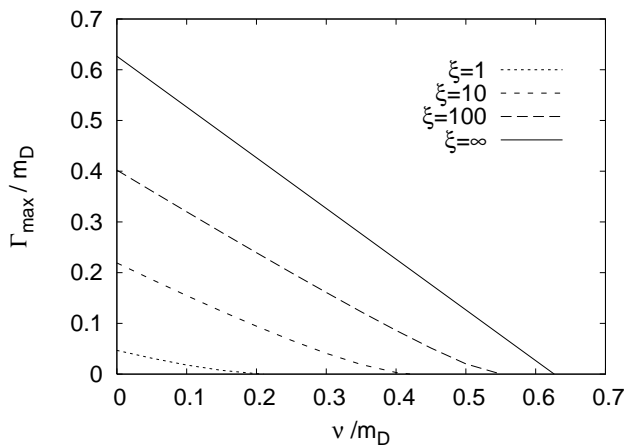


FIG. 12: The maximal growth rate of the instability as a function of the collision rate ν .

first principles this makes it difficult to fix the magnitude of ν . However, since as treated here the underlying framework of Boltzmann-Vlasov is implicitly perturbative, we can attempt to fix ν perturbatively. However, even this is non-trivial since within non-abelian theories there are at least two possible collisional frequencies to be considered [33, 34, 35, 36, 37]: (1) the frequency for hard-hard scatterings which is parametrically $\nu_{\text{hard}} \sim \alpha_s^2 \log \alpha_s^{-1}$ and (2) the frequency for hard-soft scattering which is parametrically $\nu_{\text{soft}} \sim \alpha_s \log \alpha_s^{-1}$.

The hard-hard scatterings correspond to interactions which change the momentum of a hard particle by $\mathcal{O}(p_{\text{hard}})$ and therefore represent truly momentum-space isotropizing interactions. On the other hand the hard-soft scatterings correspond to changes in momentum which are order $\mathcal{O}(gp_{\text{hard}})$. These small angle scatterings occur rather frequently and it turns out that after traversing one hard scattering mean free path, $\lambda_{\text{hard}} \sim \nu_{\text{hard}}^{-1}$, the typical deflection of the particle is also $\mathcal{O}(1)$.² The physics of small-angle scattering by the soft-background is precisely what is captured by the hard-loop treatment. However, the hard-loop framework doesn't explicitly take into account that ν_{soft} is also the frequency at which there are color-rotating interactions of the hard particles themselves. One would expect that color-rotation of the hard particles to have a larger effect on the growth of instabilities than the momentum-space isotropization via hard-hard scattering. That being said, the form of the BGK scattering kernel does not mix color channels and in that sense cannot be used to describe the physics of color-rotation of the hard particles. For this reason one is lead to the conclusion that when using the BGK kernel the appropriate damping rate is $\nu \sim \nu_{\text{hard}} \sim \alpha_s^2 \log \alpha_s^{-1}$. This conclusion for the parametric dependence of ν is also supported by looking at the leading order result for the

² This, in the end, is the source of the logarithm in ν_{hard} above.

shear viscosity [38].

Even with this conclusion it is hard to say anything quantitative about ν since the overall coefficient and the coefficient in the logarithm are not specified by such a parametric relation. One could hope that previous calculations contained in [38] of parton interaction rates could be of some use. Unfortunately, for a purely gluonic plasma it was found $\nu = 5.2 \alpha_s^2 T \log(0.25 \alpha_s^{-1})$, which clearly cannot be trusted for the values of α_s which are relevant for heavy-ion collisions ($\alpha_s \sim 0.2 - 0.4$) since ν becomes negative for large α_s . We note here that the negativity of this result at large couplings most likely stems from the strict perturbative expansion of the integrals involved failing when the hard and soft scales become comparable in magnitude. Similar erroneous negative values also occur in the perturbative expressions for heavy-quark collisional energy loss [39] when extrapolated to large coupling. A corrected calculational method which yields positive-definite results for the heavy-quark energy loss was detailed in Refs. [40, 41].

Ideally, one would revisit the calculation of the interaction rate and improve upon the techniques used where necessary. Short of such a calculation one cannot say with certainty what the numerical value of ν should be and the best we can do is to play “games”. For instance, one could insert a one into the logarithm appearing in ν similar to what other authors have done [42] to obtain $\nu \sim 5.2 \alpha_s^2 T \log(1 + 0.25 \alpha_s^{-1}) \sim 0.1 - 0.2 m_D$ for $\alpha_s = 0.2 - 0.4$. Using this admittedly specious expression for large-coupling one can expand and obtain $\lim_{\alpha_s \rightarrow \infty} \nu/m_D \sim 0.37 \alpha_s^{1/2}$. Note that in the case $N_f = 2$ both ν and m_D increase; however, the ratio of these two scales is still in the range quoted for $N_f = 0$. The range, $\nu = 0.1 - 0.2 m_D$, places us well below the threshold needed to turn off instabilities in the case of extremely anisotropic distribution functions but does imply (see Fig. 12) that for moderately small anisotropies, $\xi \sim 1$, and large coupling that it is possible for collisional damping to eliminate the unstable modes from the spectrum completely. Of course, in the limit of asymptotically small couplings the ratio ν/m_D approaches zero and the collisionless results hold to very good approximation. In the opposite limit of strong coupling the estimates here are at best guesswork and it is indeed possible that the ratio ν/m_D is larger than the range we have quoted. For example, the recent work of Peshier [43, 44] implies that ν/m_D could be as large as 0.5; however, this number results from a fit of a model assumption to lattice data and is not directly comparable to the collisional widths considered here since in their description the gluon width was assumed to be parametrically given by ν_{soft} .

Additionally, we have to mention the caveat that all the estimates above rely on full equilibrium thermal field theory calculations. For the very initial state of the matter created in an ultrarelativistic heavy-ion collision the system is clearly not in equilibrium and it is not clear how this estimate will change as a result. However, it is of crucial importance to attempt to estimate the scattering rate in a non-equilibrium setting.

IX. CONCLUSIONS

In this paper we have studied the effects of including a BGK collision kernel on the collective modes of a QCD plasma which has a hard particle distribution function which is anisotropic in momentum space. To simplify the analysis we have specialized to gluonic collective modes which have their momentum vector, \mathbf{k} , directed along the anisotropy direction, $\hat{\mathbf{n}}$. The reasons for doing this were two-fold: (1) in the collisionless limit these modes correspond to the modes which are the most unstable and (2) when $\hat{\mathbf{k}} \parallel \hat{\mathbf{n}}$ it is possible to obtain analytic expressions, Eqs. (39) and (40), for the soft-gluon self-energy structure functions. We have presented herein dispersion relations for both the stable and unstable modes in the case that there is a finite collisional frequency (or damping coefficient), ν . Our results confirm what can be expected intuitively, namely that the addition of collisional damping slows down the rate of growth of the unstable modes.

However, going beyond this intuitive expectation we have presented detailed calculations of the dependence of the maximal unstable mode growth rate on the parameter ν as shown in Fig. 12. For all values of the anisotropy parameter, ξ , we find that there is a critical value of ν_{max} above which no instability is present in the system. In Fig. 12 this corresponds to the value of ν at which the maximal growth rate vanishes. In the limit that $\xi \rightarrow \infty$ we were able to derive an analytic expression for ν_{max} , Eq. (46), finding that it corresponds precisely to the maximal growth rate obtained in the collisionless limit.

In addition, we have investigated the non-trivial analytic structure of the soft-gluon propagator in this model finding that the stable longitudinal mode becomes spacelike³ and only remains on the physical Riemann sheet up to a certain critical momentum. Beyond this critical momentum the solution goes through the logarithmic cut to the $N = -1$ Riemann sheet. For weak-damping the longitudinal mode then continues to spiral around the logarithmic branch point onto lower and lower Riemann sheets as its momentum increases (see Figs. 5a and 6a and Figs 5b and 6b). In the case of stronger anisotropies the longitudinal mode solution no longer “spirals down” the logarithmic branch

³ In the sense that $\text{Re}(\omega_L/k) < 1$.

point to lower Riemann sheets but instead simply moves lower in the complex plane of the $N = -1$ Riemann sheet (see Figs. 5c and 6c). We note that even in the isotropic case, the detailed analytic structure of the collisionally damped modes enables one to calculate quantities such as the QCD pressure including the effects of damping of the quasiparticle modes which could be of some interest [43, 44, 45, 46, 47, 48].

In the discussions section of the manuscript we have attempted to fix a numerical value for the collisional frequency ν . We have argued that since the BGK kernel does not rotate the color of the hard particles that the appropriate frequency is parametrically given by the time scale for hard-hard collisions, namely $\nu \sim \alpha_s^2 \log \alpha_s^{-1}$. Going further than this parametric estimate to a value applicable at couplings expected to be generated during heavy-ion collisions ($\alpha_s \sim 0.2 - 0.4$) is problematic due to the small coefficient which appears in the logarithm resulting in ν becoming negative. Playing a game by adding a one in the argument of the logarithm we found that $\nu \sim 0.1 - 0.2 m_D$ which according to the results of this paper would imply that for weak anisotropies there are no instabilities (see Fig. 12). For stronger anisotropies the results contained here tell us how much the maximal growth rate of the unstable modes is affected by the inclusion of collisional damping via a BGK kernel. Looking forward more detailed calculations of collision rates in a time-evolving soft-field background and true non-equilibrium situation are clearly needed.

Acknowledgements

We would like to thank Peter Arnold and Stanislaw Mrowczynski for useful discussions.

APPENDIX A: ANALYTICAL SOLUTION OF THE LINEARIZED TRANSPORT EQUATIONS

We briefly sketch how the result Eq. (13) emerges from the transport equation (12). From Eq. (12) we immediately get

$$(-i\omega + i\mathbf{v} \cdot \mathbf{k} + \nu)\delta f^i(p, K) = -g\theta_i V_\mu F^{\mu\nu}(K)\partial_\nu^{(p)} f^i(\mathbf{p}) + \nu(f_{\text{eq}}^i(\mathbf{p}) - f^i(\mathbf{p})) + \nu \frac{f_{\text{eq}}^i(\mathbf{p})}{N_{\text{eq}}} \int_{\mathbf{p}'} \delta f^i(p', K), \quad (\text{A1})$$

where $\delta f^i(p, K)$ and $F^{\mu\nu}(K)$ are the Fourier-transforms of $\delta f^i(p, X)$ and $F^{\mu\nu}(X)$, respectively. This yields

$$\delta f^i(p, K) = \frac{-ig\theta_i V_\mu F^{\mu\nu}(K)\partial_\nu^{(p)} f^i(\mathbf{p}) + i\nu(f_{\text{eq}}^i(\mathbf{p}) - f^i(\mathbf{p})) + i\nu f_{\text{eq}}^i(\mathbf{p}) \left(\int_{\mathbf{p}'} \delta f^i(p', K) \right) / N_{\text{eq}}}{\omega - \mathbf{v} \cdot \mathbf{k} + i\nu}. \quad (\text{A2})$$

Defining

$$\delta f_0^i(p, K) = \left(-ig\theta_i V_\mu F^{\mu\nu}(K)\partial_\nu^{(p)} f^i(\mathbf{p}) + i\nu(f_{\text{eq}}^i(\mathbf{p}) - f^i(\mathbf{p})) \right) D^{-1}(K, \mathbf{v}, \nu), \quad (\text{A3})$$

with $D(K, \mathbf{v}, \nu) = \omega - \mathbf{k} \cdot \mathbf{v} + i\nu$ we can write

$$\begin{aligned} \delta f^i(p, K) &= \delta f_0^i(p, K) + i\nu D^{-1}(K, \mathbf{v}, \nu) \frac{f_{\text{eq}}^i(\mathbf{p})}{N_{\text{eq}}} \int_{\mathbf{p}'} \delta f_0^i(p', K) \\ &\quad + i\nu D^{-1}(K, \mathbf{v}, \nu) \frac{f_{\text{eq}}^i(\mathbf{p})}{N_{\text{eq}}} \frac{i\nu}{N_{\text{eq}}} \int_{\mathbf{p}'} f_{\text{eq}}^i(\mathbf{p}') D^{-1}(K, \mathbf{v}', \nu) \int_{\mathbf{p}''} \delta f_0^i(p'', K) \\ &\quad + \dots \end{aligned} \quad (\text{A4})$$

Using the shorthand notation

$$\eta(K) = \int_{\mathbf{p}} \delta f_0^i(p, K) \quad (\text{A5})$$

and

$$\lambda(K, \nu) = \frac{i\nu}{N_{\text{eq}}} \int_{\mathbf{p}} f_{\text{eq}}^i(\mathbf{p}) D^{-1}(K, \mathbf{v}, \nu) \quad (\text{A6})$$

we finally have

$$\begin{aligned}\delta f^i(p, K) &= \delta f_0^i(p, K) + i\nu D^{-1}(K, \mathbf{v}, \nu) \frac{f_{\text{eq}}^i(\mathbf{p})}{N_{\text{eq}}} \eta(K) (1 + \lambda + \lambda^2 + \dots) \\ &= \delta f_0^i(p, K) + i\nu D^{-1}(K, \mathbf{v}, \nu) \frac{f_{\text{eq}}^i(\mathbf{p})}{N_{\text{eq}}} \eta(K) \frac{1}{1 - \lambda},\end{aligned}\tag{A7}$$

which translates to the final result for the current (13) by using

$$J_{\text{ind } a}^{\mu i}(K) = g \int_{\mathbf{p}} V^{\mu} \delta f_a^i(p, K),\tag{A8}$$

where we reintroduced the color indices.

-
- [1] U. W. Heinz and P. F. Kolb (2002), hep-ph/0204061.
 - [2] U. W. Heinz, Nucl. Phys. **A721**, 30 (2003), nucl-th/0212004.
 - [3] M. Gyulassy and L. McLerran, Nucl. Phys. **A750**, 30 (2005), nucl-th/0405013.
 - [4] M. H. Thoma, J. Phys. **G31**, L7 (2005), hep-ph/0409213.
 - [5] M. H. Thoma, J. Phys. **G31**, 539 (2005), hep-ph/0503154.
 - [6] D. Kharzeev and K. Tuchin, Nucl. Phys. **A753**, 316 (2005), hep-ph/0501234.
 - [7] Z. Xu and C. Greiner, Phys. Rev. **C71**, 064901 (2005), hep-ph/0406278.
 - [8] S. Mrowczynski, Phys. Lett. **B314**, 118 (1993).
 - [9] S. Mrowczynski, Phys. Rev. **C49**, 2191 (1994).
 - [10] S. Mrowczynski, Phys. Lett. **B393**, 26 (1997), hep-ph/9606442.
 - [11] S. Mrowczynski and M. H. Thoma, Phys. Rev. **D62**, 036011 (2000), hep-ph/0001164.
 - [12] M. C. Birse, C.-W. Kao, and G. C. Nayak, Phys. Lett. **B570**, 171 (2003), hep-ph/0304209.
 - [13] J. Randrup and S. Mrowczynski, Phys. Rev. **C68**, 034909 (2003), nucl-th/0303021.
 - [14] P. Romatschke and M. Strickland, Phys. Rev. **D68**, 036004 (2003), hep-ph/0304092.
 - [15] P. Arnold, J. Lenaghan, and G. D. Moore, JHEP **08**, 002 (2003), hep-ph/0307325.
 - [16] P. Romatschke and M. Strickland, Phys. Rev. **D70**, 116006 (2004), hep-ph/0406188.
 - [17] S. Mrowczynski, A. Rebhan, and M. Strickland, Phys. Rev. **D70**, 025004 (2004), hep-ph/0403256.
 - [18] A. Dumitru and Y. Nara, Phys. Lett. **B621**, 89 (2005), hep-ph/0503121.
 - [19] C. Manuel and S. Mrowczynski, Phys. Rev. **D72**, 034005 (2005), hep-ph/0504156.
 - [20] P. Arnold, G. D. Moore, and L. G. Yaffe, Phys. Rev. **D72**, 054003 (2005), hep-ph/0505212.
 - [21] A. Rebhan, P. Romatschke, and M. Strickland, JHEP **09**, 041 (2005), hep-ph/0505261.
 - [22] P. Romatschke and R. Venugopalan (2005), hep-ph/0510121.
 - [23] S. Mrowczynski, Acta Phys. Polon. **B37**, 427 (2006), hep-ph/0511052.
 - [24] E. Weibel, Phys. Rev. Lett. **2**, 83 (1959).
 - [25] P. L. Bhatnagar, E. P. Gross, and M. Krook, Phys. Rev. **94**, 511 (1954).
 - [26] H.-T. Elze and U. W. Heinz, Phys. Rept. **183**, 81 (1989).
 - [27] J. P. Blaizot and E. Iancu, Phys. Rev. Lett. **70**, 3376 (1993), hep-ph/9301236.
 - [28] P. F. Kelly, Q. Liu, C. Lucchesi, and C. Manuel, Phys. Rev. **D50**, 4209 (1994), hep-ph/9406285.
 - [29] J.-P. Blaizot and E. Iancu, Nucl. Phys. **B557**, 183 (1999), hep-ph/9903389.
 - [30] J.-P. Blaizot and E. Iancu, Phys. Rept. **359**, 355 (2002), hep-ph/0101103.
 - [31] C. Manuel and S. Mrowczynski, Phys. Rev. **D70**, 094019 (2004), hep-ph/0403024.
 - [32] M. E. Carrington, T. Fugleberg, D. Pickering, and M. H. Thoma, Can. J. Phys. **82**, 671 (2004), hep-ph/0312103.
 - [33] P. Arnold, G. D. Moore, and L. G. Yaffe, JHEP **01**, 030 (2003), hep-ph/0209353.
 - [34] A. Selikhov and M. Gyulassy, Phys. Lett. **B316**, 373 (1993), nucl-th/9307007.
 - [35] D. Bodeker, Phys. Lett. **B426**, 351 (1998), hep-ph/9801430.
 - [36] P. Arnold, D. T. Son, and L. G. Yaffe, Phys. Rev. **D59**, 105020 (1999), hep-ph/9810216.
 - [37] D. Bodeker, Nucl. Phys. **B559**, 502 (1999), hep-ph/9905239.
 - [38] M. H. Thoma, Phys. Rev. **D49**, 451 (1994), hep-ph/9308257.
 - [39] E. Braaten and M. H. Thoma, Phys. Rev. **D44**, 2625 (1991).
 - [40] P. Romatschke and M. Strickland, Phys. Rev. **D69**, 065005 (2004), hep-ph/0309093.
 - [41] P. Romatschke and M. Strickland, Phys. Rev. **D71**, 125008 (2005), hep-ph/0408275.
 - [42] J. I. Kapusta, P. Lichard, and D. Seibert, Phys. Rev. **D44**, 2774 (1991).
 - [43] A. Peshier, Phys. Rev. **D70**, 034016 (2004), hep-ph/0403225.
 - [44] A. Peshier and W. Cassing, Phys. Rev. Lett. **94**, 172301 (2005), hep-ph/0502138.
 - [45] J. O. Andersen, E. Braaten, and M. Strickland, Phys. Rev. Lett. **83**, 2139 (1999), hep-ph/9902327.

- [46] J. O. Andersen, E. Braaten, and M. Strickland, Phys. Rev. **D61**, 014017 (2000), hep-ph/9905337.
- [47] J. O. Andersen, E. Braaten, E. Petitgirard, and M. Strickland, Phys. Rev. **D66**, 085016 (2002), hep-ph/0205085.
- [48] J. O. Andersen, E. Petitgirard, and M. Strickland, Phys. Rev. **D70**, 045001 (2004), hep-ph/0302069.